

RESEARCH

Open Access



Comparative pathogenicity of influenza virus-induced pneumonia mouse model following intranasal and aerosolized intratracheal inoculation

Xiu-Yu Jin^{1†}, Hui-Ying Yang^{2†}, Guang-Yu Zhao², Chen-Xi Dai², Zai-Qing Zhang², Dong-Sheng Zhou², Qi Yin^{2*} and Er-Hei Dai^{1*}

Abstract

Background Infection of mice with mouse-adapted strains of influenza virus has been widely used to establish mouse pneumonia models. Intranasal inoculation is the traditional route for constructing an influenza virus-induced pneumonia mouse model, while intratracheal inoculation has been gradually applied in recent years. In this article, the pathogenicity of influenza virus-induced pneumonia mouse models following intranasal and aerosolized intratracheal inoculation were compared.

Methods By comparing the two ways of influenza inoculation, intranasal and intratracheal, a variety of indices such as survival rate, body weight change, viral titer and load, pathological change, lung wet/dry ratio, and inflammatory factors were investigated. Meanwhile, the transcriptome was applied for the initial exploration of the mechanism underlying the variations in the results between the two inoculation methods.

Results The findings suggest that aerosolized intratracheal infection leads to more severe lung injury and higher viral loads in the lungs compared to intranasal infection, which may be influenced by the initial site of infection, sialic acid receptor distribution, and host innate immunity.

Conclusion Intratracheal inoculation is a better method for modelling severe pneumonia in mice than intranasal infection.

Keywords Influenza, Aerosolization, Intratracheal, Intranasal, Mice

[†]Xiu-Yu Jin and Hui-Ying Yang have contributed equally to this work.

*Correspondence:

Qi Yin

jnyzyinqi@163.com

Er-Hei Dai

daieh2008@126.com

¹Hebei Key Laboratory of Immune Mechanism of Major Infectious Diseases and New Technology of Diagnosis and Treatment, The Fifth Hospital of Shijiazhuang, Shijiazhuang, People's Republic of China

²State Key Laboratory of Pathogen and Biosecurity, Beijing Institute of Microbiology and Epidemiology, Academy of Military Medical Sciences, Beijing 100071, China



Introduction

Influenza virus, a prevalent respiratory pathogen, poses a serious threat to human health and healthcare systems due to its widespread transmission and high mortality rates on a global scale each year. The World Health Organization (WHO) estimates that approximately one billion individuals contract seasonal influenza annually, with 3–5 million cases classified as severe [1, 2]. Certain populations, such as young children, the elderly, pregnant women, individuals with chronic illnesses, and those with compromised immune systems, are particularly susceptible to infection by the influenza virus [3–5]. In certain instances, influenza virus epidemics may result in serious complications and even death [6, 7].

Reliable animal models are solid foundations for influenza-related basic and applied research. Small mammals are crucial in the construction of influenza virus pneumonia models [8, 9]. While established models utilizing ferrets and guinea pigs exist, mice are preferred by researchers for their cost-effectiveness and ease of management [10–12].

In the process of mouse model construction, intranasal and intratracheal inoculation are two common approaches employed to simulate the infection process. Intranasal inoculation is characterized by simplicity and suitability for large-scale experiments, but results may vary depending on the manipulations of researchers [13]. In contrast, intratracheal inoculation allows for precise administration of the virus to a precise anatomical location, making it a more targeted approach compared to intranasal inoculation [14]. The aerosolized intratracheal inoculation offers advantages in terms of non-invasiveness, reduction of liquid particle size, and increased lung deposition rates, thereby contributing to more precise modelling of infection pathways and pathological processes. The MicroSprayer (Huironghe Company, Beijing, China) allows for the aerosolization of influenza virus solution to directly target the lungs and closely replicate the natural process of human infection [15–18].

In this study, C57BL/6J mice were employed to construct an influenza-infected model [19]. The aim was to compare the different pathogenic phenotypes, disease progression, and other relevant factors resulting from two distinct methods of inoculation (intranasal inoculation and aerosolized intratracheal inoculation) in the mouse model. Additionally, mechanisms that may contribute to these observed variances were investigated.

Materials and methods

Mice and virus

Eight-week-old, wild-type, female C57BL/6J mice (Vital River Laboratory, Beijing, China) were housed in specific-pathogen-free conditions and provided with ad libitum access to food and water. The animal experiments

were approved by the Animals Ethics Committee of the Academy of Military Medical Sciences (approval no. IACUC-DWZX-2023-008).

Mouse-adapted influenza A/Puerto Rico/8/34 (H1N1) (PR8) [20] was cultured in chick embryos, and the virus-containing allantoic fluid was harvested and stored in aliquots at -80 °C.

Aerosolization of influenza virus solutions

Influenza virus aerosolization was accomplished with a MicroSprayer (Huironghe Company, Beijing, China). Anesthetized mice were fixed on the operating table, and a laryngoscope was inserted into the deep oral cavity to expose the vocal fold. Then the needle of the MicroSprayer was inserted into the trachea for rapid injection to achieve aerosolization of influenza virus. The mean mass aerodynamic diameter (MMAD) of the influenza virus aerosol particles was determined using an aerodynamic particle sizer (APS 3321, TSI, USA) with a sampling time of 15 s and a sampling flow rate of 5 L/min. The experiment was repeated three times.

Aerosol distribution of Trypan Blue and cyanine dye

Mice were anaesthetized using a 1% pentobarbital sodium solution administered via intraperitoneal injection and immobilized on the operating table. Intranasal inoculation was performed by instilling 50 µL of Trypan Blue or Cy7.5 through one nostril of the mouse with a pipette gun attached to the tip. Trypan Blue and cyanine dye (Cy7.5) were separately sprayed into the lungs of mice using the MicroSprayer for aerosolized intratracheal inoculation. The purpose of employing Trypan Blue was to compare the distribution effects of intranasal and aerosolized intratracheal inoculation in the lungs through visual observation, and the difference in fluorescence level was presented by Cy7.5. Following the ejection of Trypan Blue, the mice were immediately executed and their lungs were extracted. In vivo imaging of the lungs was conducted using an IVIS Spectrum small-animal imaging system, employing excitation and emission wavelengths of 770/820 nm after the cyanine dye inoculation. The isolated lungs were subjected to the same imaging procedure.

Animal experimental protocol

C57BL/6J mice were divided into two groups and were respectively inoculated with influenza virus by intranasal or aerosolized intratracheal inoculation, with virus titer of 4.6 PFU, 83.8 PFU, 420 PFU, and 1790 PFU. Lung tissues were removed for histopathological assay, and viral titer and viral load detection was performed at 1, 3, and 5 days post-infection (dpi). Alveolar lavage fluid was collected for cytokine ELISA assays at 1, 3, and 5 dpi. Lung

wet/dry ratio was assessed at 1, 3, and 5 dpi and transcriptome analysis was conducted at 5 dpi.

Plaque assay and viral load

Mice that were subjected to the aforementioned treatment were euthanized, and their lungs were surgically removed and placed in 1 mL DMEM at 1, 3, and 5 dpi. The lung tissues were then homogenized and centrifuged at 12,000 rpm for 10 min, repeated twice, to obtain the supernatant. The supernatant was subsequently filtered through a 0.22 μ m filter. MDCK cells were utilized to assess the viral titer of the supernatant. Total RNA was extracted from 200 μ L supernatant using a PureLink™ RNA Mini Kit (12183018 A, Thermo Fisher), followed by Q-PCR to detect viral load, with a nucleic acid upload of 100 ng, using primers NP-forward, 5'-GACCRATCCTGTCACCTCTGAC-3'; NP-reverse, 5'-GGGCATTYTGACAAAKCGTCTACG-3'; NP-probe, TGCAGTCCTC GCTCACTGGCAG.

Histopathological assay

Following intranasal and aerosolized intratracheal infection of C57BL/6J with PR8, the mice were euthanized and the lungs were removed at the indicated time points. The lung tissues were fixed by immersion in a 4% formalin for at least 1 day. Subsequently, the tissues were embedded in paraffin to form paraffin blocks, which were then sectioned and stained with hematoxylin and eosin. The histopathology score was primarily determined by assessing the degree of alveolar wall thickening, inflammatory cell infiltration, perivascular edema, haemorrhage, and bruising through a 4-point scoring system [21]. The more severe the above lesion, the higher the histopathological score.

Lung wet/dry ratio

The wet/dry ratio of the lungs was applied to estimate pulmonary edema. On days 1, 3, and 5 post-challenge, the right lung tissues were excised, dried with a clean paper towel, and instantly weighed for wet lung weight (W), followed by incubation of the lungs at 80 °C for 48 h to acquire dry weight (D). Ultimately, the lung W/D ratio was calculated.

ELISA

Bronchoalveolar lavage fluid (BALF) was collected at 1, 3, and 5 dpi. The BALF was obtained by instilling 800 μ L PBS into the trachea of mice, followed by three repeated lavages. The collected fluid was then transferred into 1.5 mL EP tubes and centrifuged at 4 °C for 10 min at 3000 g. The concentration of cytokines in the BALF was determined using a mouse ELISA kit (Solarbio, Beijing, China) in accordance with the provided instructions. The ELISA

assay included the measurement of IL-6, IL-17 A, MPO, ICAM-1, and IL-1 β .

RNA extraction, library preparation and sequencing

TRIzol Reagent (Invitrogen, USA) was used to extract total RNA from lung tissues [22]. After RNA extraction, DNase I was used to carry out DNA digestion. Utilizing a Nanodrop™ One C Spectrophotometer (Thermo Fisher Scientific Inc.), A260/A280 values were examined to assess the purity of the RNA. RNA Integrity was confirmed by 1.5% agarose gel electrophoresis. Qubit3.0 was implemented to quantify the qualified RNAs using the Qubit™ RNA Broad Range Assay kit (Life Technologies, Q10210). As directed by the manufacturer, 2 μ g total RNAs were used to prepare the stranded RNA sequencing library using the KCTM Stranded mRNA Library Prep Kit for Illumina®. 200–500 bps PCR products were enriched, quantified, and then sequenced on a DNBSEQ-T7 sequencer with PE150 model.

RNA-Seq data analysis

First, low-quality reads were removed and reads tainted with adaptor sequences were trimmed from the raw sequencing data using Trimmomatic. With STRA software and default parameters, clean data were mapped to the mouse reference genome. Following the count of reads mapped to each gene's exon regions using featureCounts, RPKMs were determined. The edgeR software was used to identify genes that were expressed differently between groups. The statistical significance of variations in gene expression was assessed using a fold-change criteria of two and a *p*-value cutoff of 0.05. KOBAS software was implemented to perform gene ontology (GO) analysis and Kyoto encyclopedia of genes and genomes (KEGG) enrichment analysis for differentially expressed genes (DEGs). A *p*-value limit of 0.05 was used to determine statistically significant enrichment. Using rMATS with a 0.05 FDR value threshold and a 0.05 absolute value of $\Delta\psi$, alternative splicing events were found.

Statistical analysis

All data were analysed with GraphPad Prism 8.0 software. Unless specified, the data are presented as the mean \pm SD in all experiments. Comparisons between

survival curves were analyzed using the log-rank test. Except for survival analysis, analysis of variance (ANOVA) was used to determine statistical significance between two groups at multiple time points, and t-test was used to analyze statistical differences between the two groups (n.s., not significant; *, *P*<0.05; **, *P*<0.01; ***, *P*<0.001).

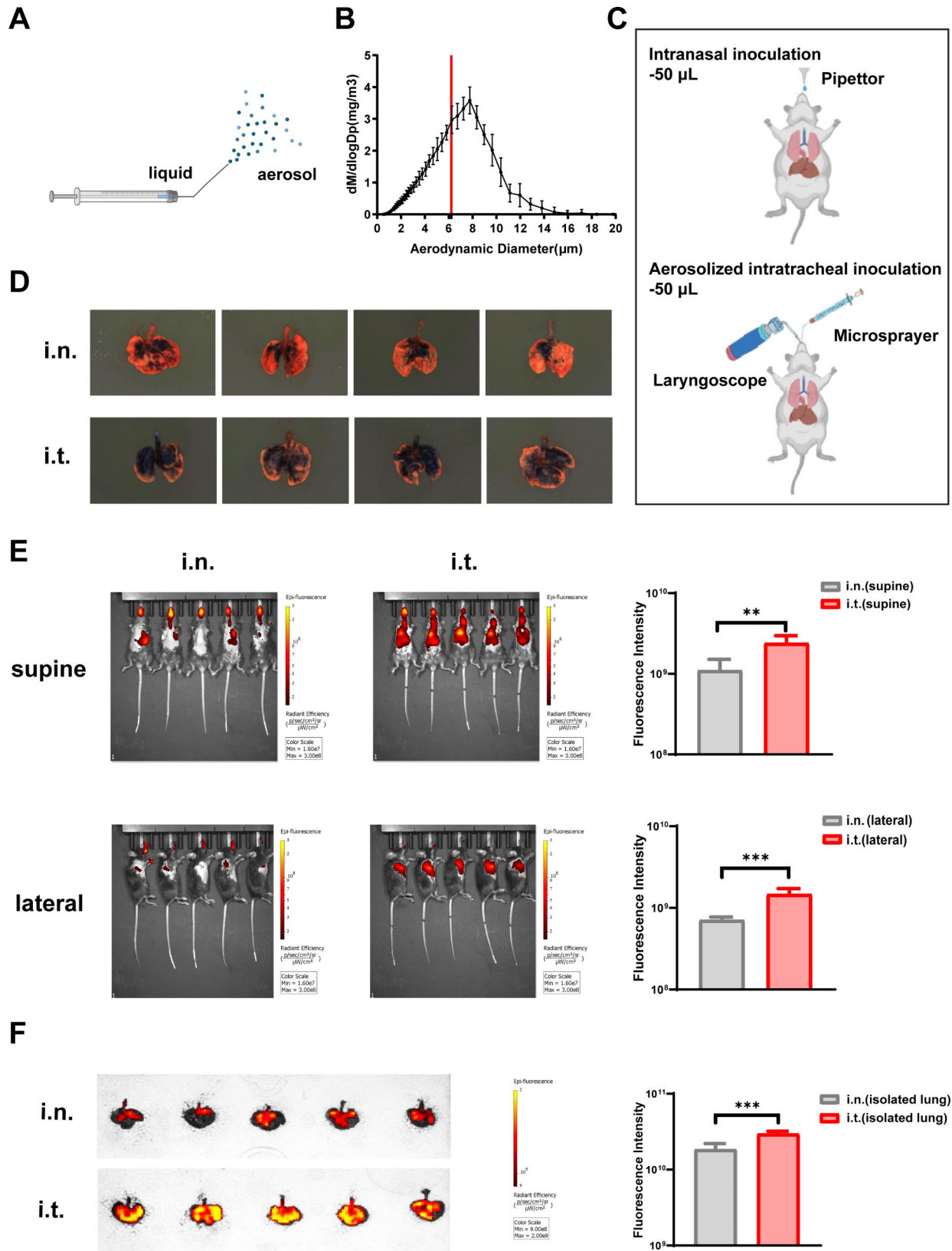


Fig. 1 (See legend on next page.)

(See figure on previous page.)

Fig. 1 Characterization of influenza virus aerosolization. **(A)** Physical diagram of nebulizer (Created with bioRender.com). **(B)** The mean mass aerodynamic diameter of the influenza virus liquid nebulized by the MicroSprayer as calculated by aerodynamic particle sizer. **(C)** Schematic diagrams of intranasal (i.n.) and aerosolized intratracheal (i.t.) inoculation. **(D)** Trypan Blue was inoculated into mouse lungs by intranasal (top) and intratracheal (bottom) inoculation, respectively ($n=4$ per group). **(E-F)** Cyanine dye was inoculated into mouse lungs either by intranasal and intratracheal inoculation ($n=5$ per group), and images were taken under IVIS Spectrum small-animal imaging system. **(E)** The top and bottom row indicated the supine and lateral image of intranasal (left) and intratracheal (middle) mice respectively, and the corresponding comparison of fluorescence intensity was shown (right). **(F)** The left column indicated the fluorescence area of the isolated lung of intranasal (top) and intratracheal (bottom) mice, and the comparison of fluorescence intensity was shown (right). Significance was calculated by unpaired t-test (n.s., not significant; *, $P<0.05$; **, $P<0.01$; ***, $P<0.001$)

Results

The aerosolized solution is delivered to the mouse lung in a targeted and quantitative manner with a more uniform distribution

The physical diagram of the nebulizer was shown in Fig. 1A. The mean mass aerodynamic diameter of aerosolized virus particles was $6.22\pm 0.13\ \mu\text{m}$, closely aligning with the range of particles that settle in the lungs during normal human respiration (Fig. 1B) [23, 24]. The schematic of intranasal and aerosolized intratracheal inoculation was shown in Fig. 1C. Intranasal inoculation was achieved by pipetting 50 μL liquid twice into the one-sided nostril of the mice. For aerosolized intratracheal inoculation, the needle of the MicroSprayer was inserted through the mouse trachea, and a quantitative amount of liquid (50 μL) was aerosolized directly into the lungs through a rapid lever push.

To assess the particle distribution within the lungs under different inoculation methods, C57BL/6J mice were inoculated with Trypan Blue and Cy7.5, respectively. Intratracheal administration of Trypan Blue resulted in a uniform dye distribution throughout all lung lobes, encompassing a significant portion of the lungs, whereas Trypan Blue administrated intranasally primarily localized at the junction between the lungs and the bronchi (Fig. 1D). Consistent with the above results, the mice inoculated with Cy7.5 intratracheally showed a higher fluorescence area and intensity in the lungs *in vivo* (Fig. 1E) and *ex vivo* (Fig. 1F) compared to mice received intranasal inoculation. The results indicated that aerosolized intratracheal inoculation was more effective in penetrating into the lungs of the mice and achieving uniform particle distribution compared to intranasal inoculation.

Aerosolized influenza results in higher fatality and more significant weight loss

Mice were infected by multiple doses of influenza virus by intranasal and aerosolized intratracheal inoculation. The effects of various doses on time to death and percent survival were presented in Fig. 2A. At infectious doses of 83.8 PFU and 420 PFU, the mortality both reached 100% after intratracheal inoculation, while intranasal administration resulted in death rates of 0% and 60%, respectively. Intranasal inoculated mice exhibited prolonged survival compared to intratracheal inoculated mice when administered a dose of 1790 PFU, despite both groups

ultimately reaching 100% mortality. Weight loss was observed earlier in the mice underwent intratracheal inoculation compared to those received intranasal inoculation when administered the same dosage (Fig. 2B). With the exception of 1790 PFU, the degree of weight loss in mice following intratracheal inoculation was more pronounced than that following intranasal inoculation, with a statistically significant difference observed.

Higher viral load and titer were observed upon aerosolized intratracheal inoculation

To compare the viral load and viral titer levels of the two inoculation methods, C57BL/6J mice were infected intranasally or intratracheally with 4.6 PFU, 83.8 PFU, 420 PFU, and 1790 PFU of influenza virus, respectively. Viral load was detected by applying Q-PCR to viral RNA extracted from 200 μL supernatant of grinding fluid obtained from the entire lung. MDCK cells were utilized to assess the viral titer of the supernatant from homogenized lungs. The supernatant was serially diluted by DMEM containing 1% TPCK trypsin for plaque assay. The viral load results shown in Fig. 3A indicated that at the doses of 83.8 PFU and 420 PFU, the viral load via intratracheal inoculation was significantly higher than that via intranasal inoculation. The results of the viral titer demonstrated a correlation with the viral load. Mice infected by intratracheal inoculation exhibited higher viral titers in the lungs compared to those infected via intranasal inoculation, with statistically significant differences observed (Fig. 3B).

Aerosolized influenza leads to more pronounced histopathological lesion

To compare the extent of pathological damage caused by two different virus inoculation methods, the left lungs of mice were removed at 1, 3 and 5 dpi. Pathological changes in the lungs of mice infected with multi-dose influenza virus were shown in Fig. 4A. Histopathological scores (Fig. 4B) and lung wet/dry ratio (Fig. 4C) were both higher after intratracheal inoculation than intranasal inoculation at the same viral dose.

Aerosolized influenza virus infection triggers higher levels of inflammatory factors

To assess the early immune response in infected mice, cytokines including IL-6, IL-1 β , and IL-17 A were

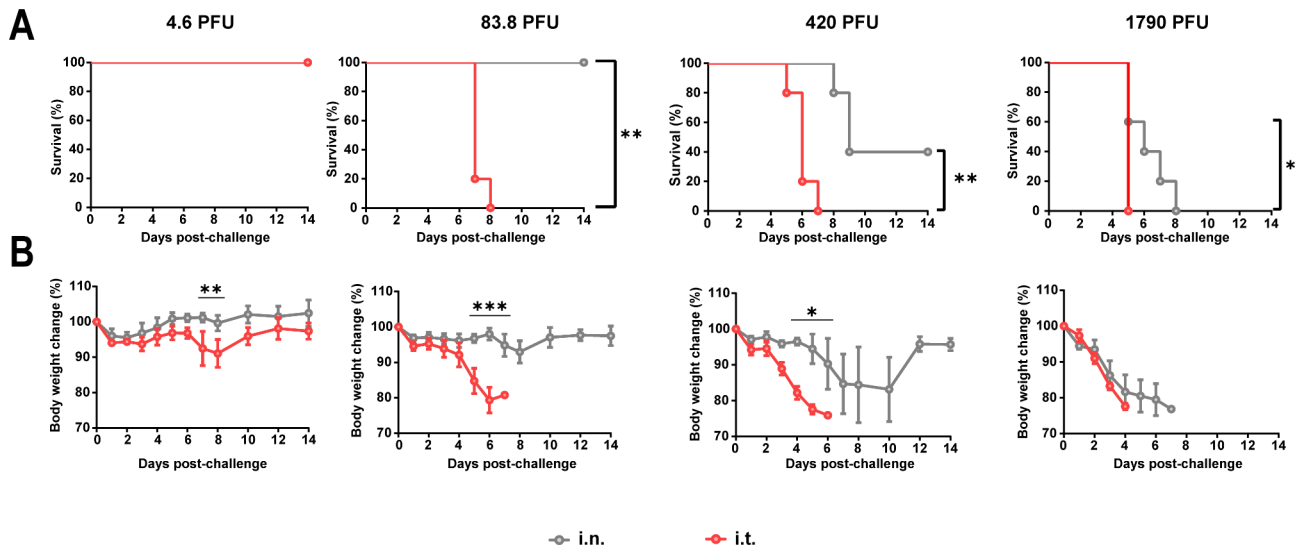


Fig. 2 Survival and weight change curve plots for multi-dose influenza viruses. (A-B) C57BL/6J mice (5 per group) were infected intranasally or intratracheally with 4.6 PFU, 83.8 PFU, 420 PFU, and 1790 PFU of influenza virus, respectively, and monitored daily for 14 days for survival (A) and weight loss (B). Any mouse which lost > 25% initial body weight was euthanized. Log-rank test or two-way ANOVA was used to determine statistical significance among different groups (n.s., not significant; *, $P < 0.05$; **, $P < 0.01$; ***, $P < 0.001$)

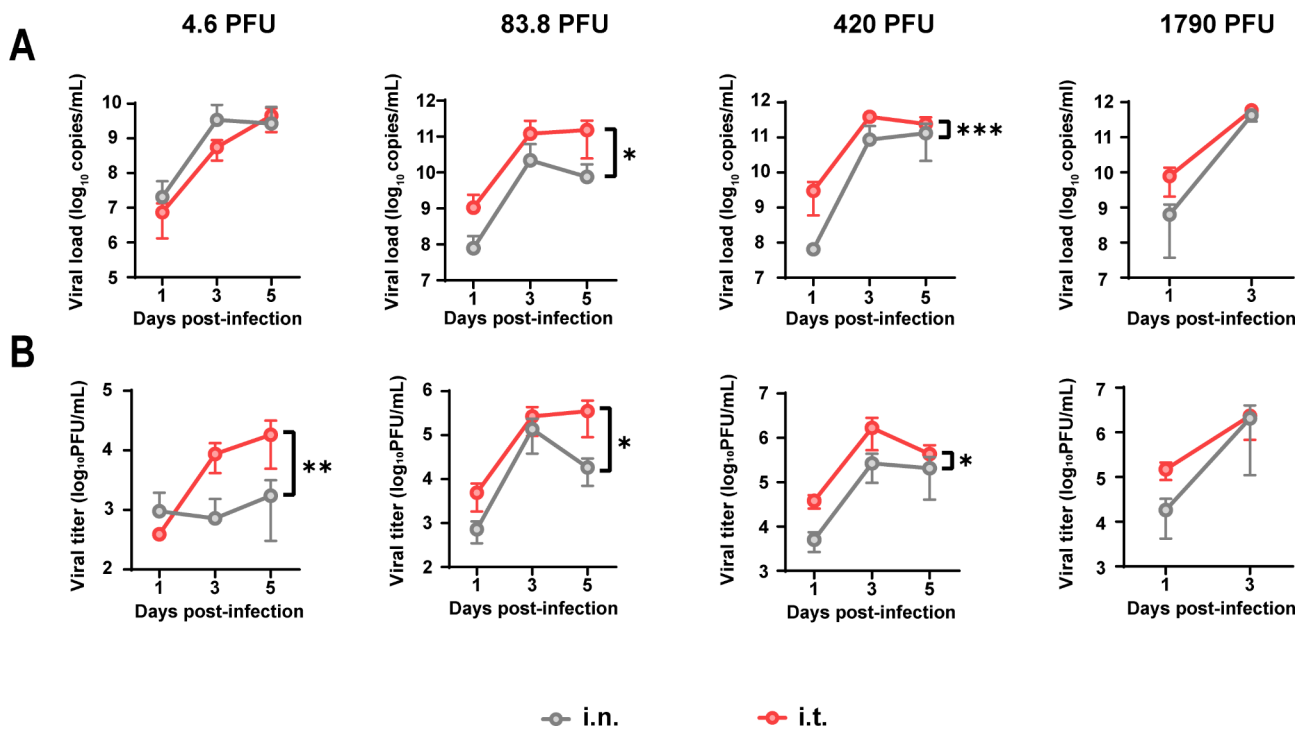


Fig. 3 Comparison of viral load and titer in mice after intranasal and aerosolized intratracheal inoculation with PR8. (A-B) C57BL/6J mice ($n = 5$ per sampling time) were inoculated with PR8 via intranasal and intratracheal inoculation, and the viral load (A) with a detection limit of 1 copy/100 ng and viral titer (B) with a detection limit of 50 PFU/mL were determined by RT-qPCR and plaque assay, respectively, at the indicated time. The infected doses in the graph from left to right are 4.6 PFU, 83.8 PFU, 420 PFU and 1790 PFU in sequence. Significance was calculated by two-way ANOVA (n.s., not significant; *, $P < 0.05$; **, $P < 0.01$; ***, $P < 0.001$)

assayed and analyzed. These pro-inflammatory factors are involved in immune cell activation and viral clearance during the influenza infection process. The mice infected via intratracheal inoculation expressed significantly

elevated levels of cytokines than those infected via intranasal inoculation (Fig. 5). Specifically, the expression level of multiple cytokines, including IL-6 and IL-17 A, increased significantly at 3 and 5 dpi in intratracheal

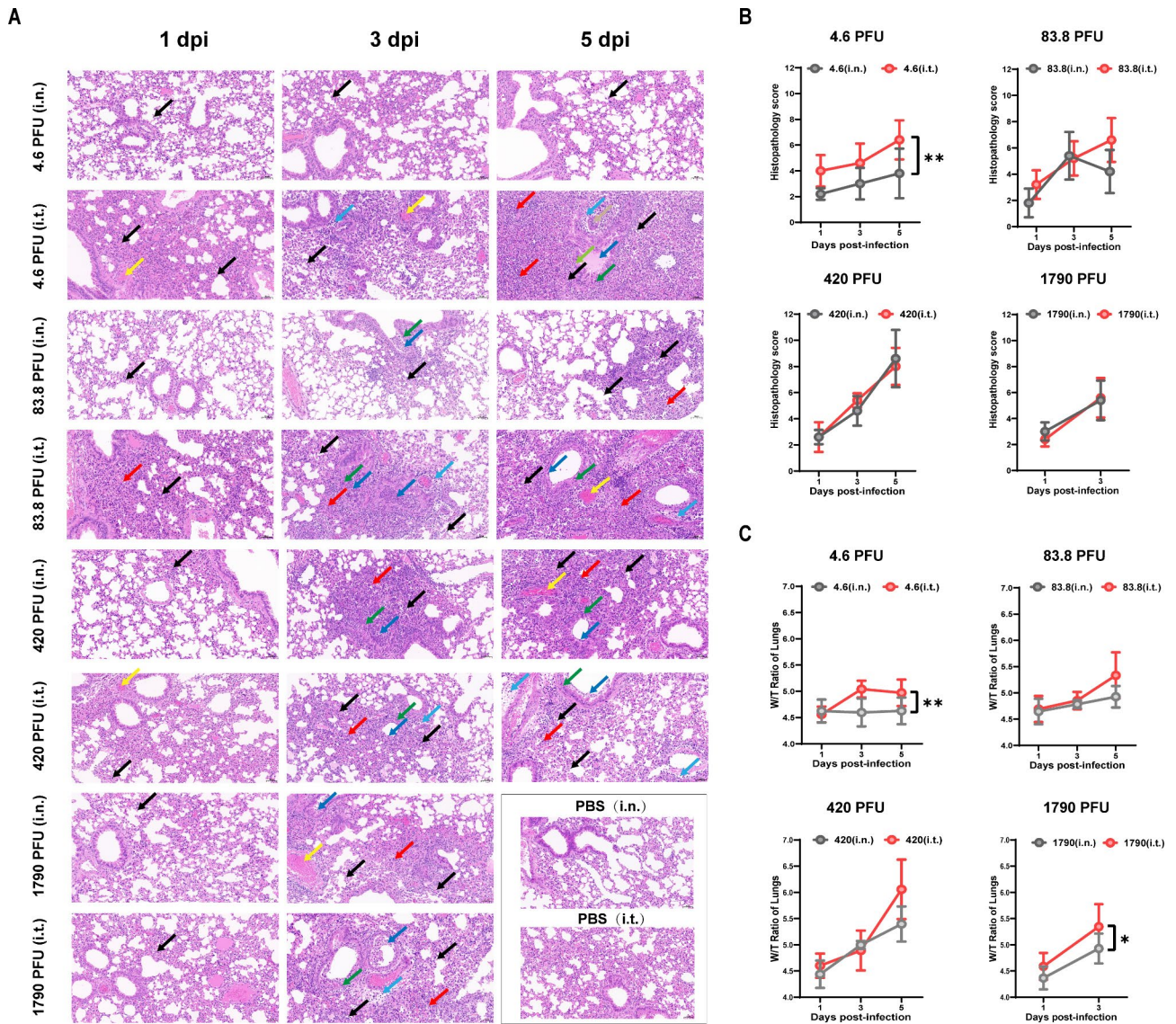


Fig. 4 Pathological analyze, pathological score and lung wet/dry ratio in mice at 1, 3 and 5 dpi ($n=5$ per group per time point). **(A)** Histopathological analysis of lung tissue in infected mice at 1,3 and 5 dpi under 200x magnification. **(B-C)** Changes in pathological scores **(B)** and lung wet/dry ratio **(C)** at 1, 3 and 5 dpi in mice infected by influenza viruses of 4.6 PFU,83.8 PFU,420 PFU and 1790 PFU, respectively. Arrows indicated lesions: black for inflammatory cell infiltration, yellow for vascular bruising, red for necrotic cellular debris of lung tissue, blue for perivascular oedema, dark blue for inflammatory cell infiltration and necrotic debris visible in the lumen of the tubes, green for eosinophilic material visible in the lumen of the alveoli, and dark for green bronchial epithelial cell necrosis. Scale bar: 50 μ m

inoculated mice compared to intranasal inoculated mice. Besides, the expression of IL-1 β increased significantly at 3 dpi. These findings demonstrated that aerosolized PR8 could induce more robust immune responses in mice. In addition to the cytokines mentioned above, the expressed levels of neutrophil myeloperoxidase (MPO) and intercellular cell adhesion molecule-1 (ICAM-1) were compared between intranasal and aerosolized intratracheal inoculation. MPO is crucial in influenza-induced severe pneumonia, as it mediates the production of a tissue-damaging factor named hypochlorous acid when released extracellularly [25]. In addition, MPO plays an important

role in the killing of microorganisms by neutrophils [26]. The lung ICAM is indispensable for innate leukocyte migration into influenza-infected lungs and long-term antiviral cellular immunity [27]. The expression levels of MPO and ICAM-1 in intratracheal inoculated mice remained higher than that in intranasal inoculated mice. These findings suggested that aerosolized influenza virus infection led to more severe tissue damage accompanied by a more intense antiviral response of the mouse organism.

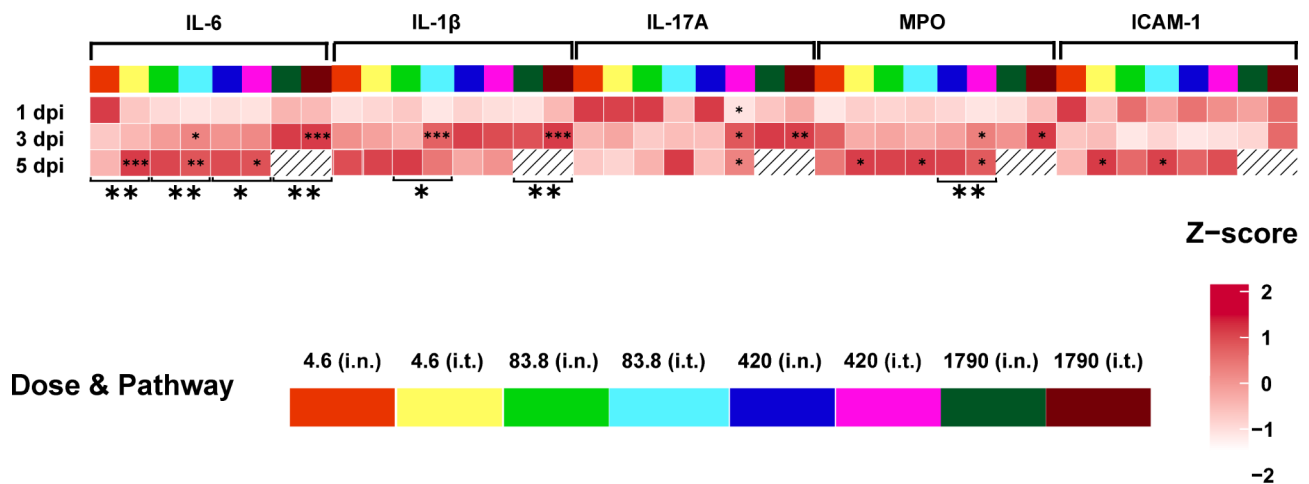


Fig. 5 Comparison of inflammatory responses in the lungs of mice ($n=5$ per group per sampling time) infected with PR8 virus intranasally or intratracheally. Comparison of inflammatory factors in PR8-infected mice in BALF: BALF was collected at the indicated times. Inflammatory factor expression was recorded as the lowest limit of detection when the value converted by substituting the OD value into the standard curve was less than the lowest limit of detection. Significance was calculated by two-way ANOVA (n.s., not significant; *, $P<0.05$; **, $P<0.01$; ***, $P<0.001$)

Intratracheal inoculation of aerosolized PR8 leads to robust innate immune responses in the lungs

To further elucidate the mechanism of the difference in transcript levels between intranasal and aerosolized intratracheal administration of the virus, the lung transcriptome of mice infected with influenza virus was determined at 5 dpi. Mice that received intranasal inoculation were designated as the control group, while those that underwent aerosolized intratracheal inoculation were assigned to the experimental group. Principal component analysis (PCA) was performed using normalized counts to assess the transcriptome data quality (Fig. 6A). The data indicated that compared to intranasal inoculation, the expression of 895 genes increased and the expression of 314 genes decreased after aerosolized intratracheal inoculation (Fig. 6B). In addition, KEGG pathway enrichment revealed differences in multiple inflammatory pathways, including the NOD-like receptor signalling pathway, JAK-STAT signalling pathway, Toll-like receptor signalling pathway, IL-17 signalling pathway, neutrophil extracellular trap formation, and other immune pathways (Fig. 6C). The findings presented above aligned with prior results indicating that intratracheal inoculation induced a more intense inflammatory response and greater pathological damage. Furthermore, GO analysis performed at the bioprocess level revealed that mice that received intratracheal inoculation exhibited enhanced leukocyte recruitment, proliferation, migration and pro-inflammatory cytokine production, along with increased expression of extracellular matrix (ECM) components, in comparison to intranasal inoculation (Fig. 6D). In comparison to intranasal inoculation, aerosolized intratracheal inoculation in mice resulted in a significant up-regulation of genes in the lungs.

Specifically, 13 genes were found to be involved in the inflammatory process, including proinflammatory factor production, neutrophil recruitment, delayed neutrophil apoptosis, and ECM protease. Additionally, 9 genes were significantly down-regulated, primarily affecting the composition of the ECM (Fig. 6E).

Discussion

Infection of mice with mouse-adapted strains of influenza virus has been widely employed to establish mouse pneumonia models. Intranasal inoculation is the traditional route for constructing an influenza virus-induced pneumonia mouse model, while intratracheal inoculation has been gradually applied in recent years. In this study, we compared two mouse models inoculated with influenza virus by intranasal or aerosolized intratracheal routes. Aerosolized intratracheal inoculation resulted in higher lethality and more rapid weight loss compared to intranasal inoculation. Additionally, intratracheal inoculation led to higher viral load and titer in the lung, accompanied by more pronounced pathological changes and a more intense inflammatory response. Similar results have been observed in ferrets. Ferrets have been shown to mimic the pathogenic mechanism of human infection with influenza most closely. Studies have shown that high morbidity and mortality in ferrets infected with low pathogenicity avian influenza viruses can be achieved by the intratracheal route [28]. And there are data suggesting that intratracheal inoculation may be more suitable for investigating influenza virus-induced lower respiratory tract disease in ferret models of influenza infection compared to intranasal inoculation [29].

It was found that the influenza virus tends to replicate at a higher level in the lungs compared to nasal tissues,

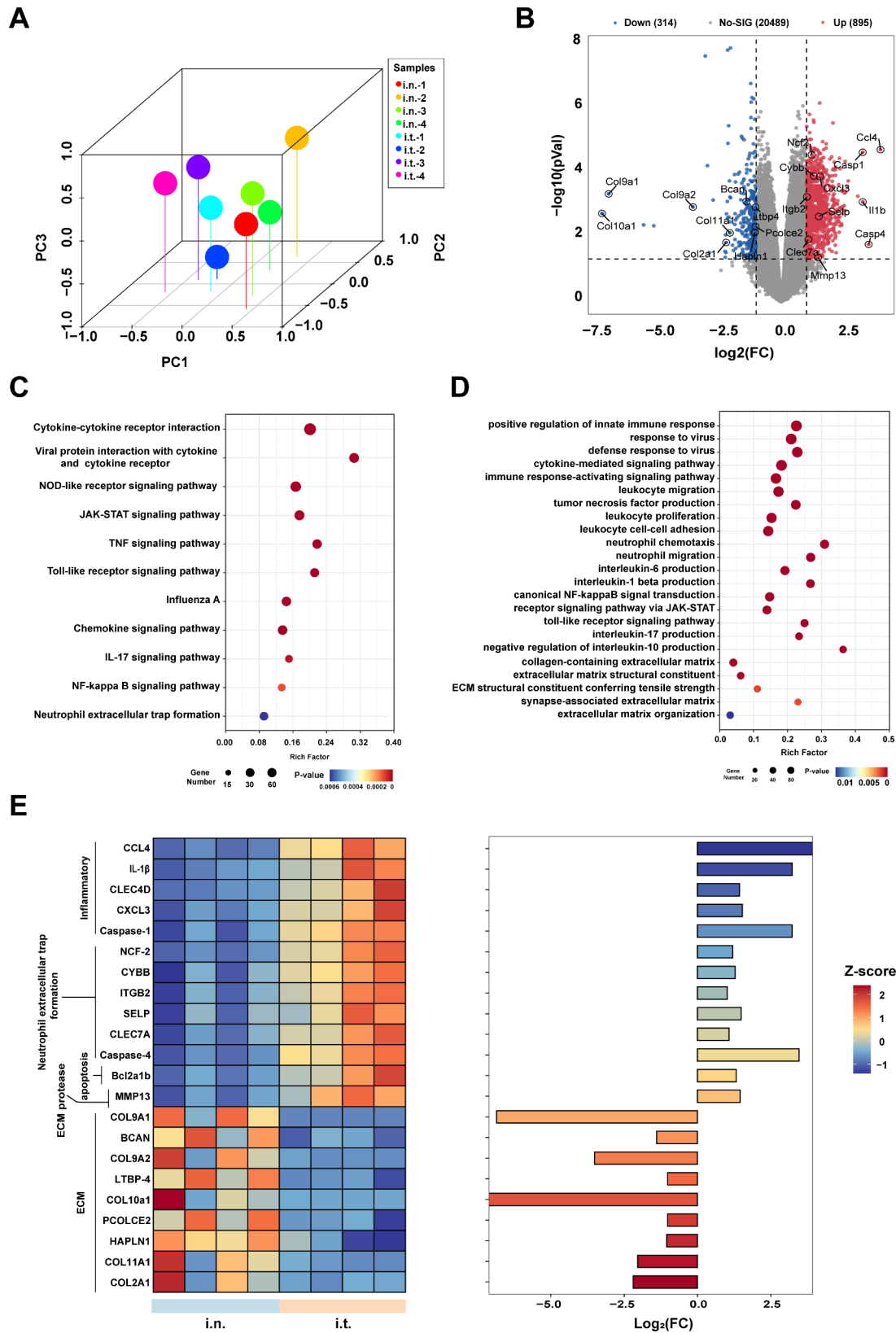


Fig. 6 (See legend on next page.)

(See figure on previous page.)

Fig. 6 DEGs in PR8-infected C57BL/6J mice after aerosolized intratracheal inoculation obtained by RNA-seq compared to intranasal inoculation. **(A)** Principal component analysis of normalized RNA sequencing results for each group. **(B)** Numbers of DEGs after aerosolized intratracheal inoculation of PR8 compared to intranasal inoculation. **(C)** Visualization of KEGG pathway enrichment of upregulated genes at 5 dpi in the intratracheally inoculated lungs. Bubble map cells are coloured according to their *p*-value. **(D)** GO terms in biological processes describing genes that are genetically up-regulated and down-regulated at 5 dpi. Bubble map cells are coloured according to their *p*-value. **(E)** Heatmap displayed the expression patterns of the associated 23 differential genes. Bar graph indicated the fold-change of the expression of the same genes in mouse lungs after aerosolized intratracheal inoculation compared to intranasal inoculation. Heatmap cells are coloured according to their Z-value

despite being inoculated via intranasal inoculation [30]. For instance, mice infected with A/Korea/01/2009 (H1N1) virus via intranasal inoculation exhibited high virus replication in lungs and low replication in nasal tissues [30]. With intranasal inoculation, the influenza virus replication initially occurred in the nasal cavity and subsequently spread to the lungs after virus shedding. That means that a reduced amount of virus reaches the distal lungs through intranasal inoculation. Intratracheal inoculation allows the influenza virus to directly reach the lungs of mice, bypassing the spreading process. Since the two inoculation methods contribute to the difference in the initial site of infection, aerosolized intratracheal inoculation ensured greater exposure of the virus to the lungs and was more stable compared to intranasal inoculation, explaining precisely why the lung viral titer and load remained higher in the intratracheally-inoculated lungs.

In addition, the distribution of sialic acid receptors varies throughout the respiratory system. It has been proved that PR8 binds preferentially to α 2,3-linked sialic acid receptor [31]. It was mentioned that it is now generally accepted that mice have more α 2,3-linked sialic acid receptors distributed in their lungs [32]. Given this, in combination with the fact that the initial site of infection is different between the two methods of inoculation, aerosolized intratracheal inoculation exposes more α 2,3-linked sialic acid receptors, which results in a higher amount of invading virus and more viral replication.

Regarding the comparison between aerosolized intratracheal inoculation and intratracheal instillation, preliminary results from other research models in our laboratory have shown that there was no significant difference in survival and pathological changes between aerosol and droplet methods of intratracheal inoculation [33]. Moreover, intratracheal instillation was prone to cause unilateral pneumonia, stress, hypoxia and even death in mice. In contrast, aerosolized intratracheal inoculation demonstrated better lung distribution, pathologic homogeneity, and reproducibility among animals. To simulate aerosolized infections, some researchers have also infected mice via animal nose-only aerosol exposure device to mimic natural inhalation [34, 35]. However, it is difficult to quantify and therefore produces inconsistent results. Aerosolized intratracheal inoculation can provide stable results, thus becoming a more adopted way of aerosolizing infected mice. Secondly, intratracheal inoculation in earlier studies was invasive [36, 37]. Aerosolized

intratracheal inoculation employed in this study was non-invasive and can be independently performed by lab researchers with minimal training. Compared to previous studies [13, 29, 38, 39], the transcriptome was applied in our study for the first time to investigate the mechanisms of intranasal and intratracheal inoculation.

As revealed by GO analysis of transcriptomes, the positive regulation of innate immunity was essential in the early stages of influenza virus infection in mice. Compared to intranasal infection, aerosolized intratracheal inoculation induced a stronger innate immune response. From the transcriptome results in Fig. 6E, “neutrophil activation” was manifested by elevated expression of genes including activated inflammatory pathways (*Ccl4*, *Il1b*, *Clec4d*, *Cxcl3*, and *Casp1*), neutrophil extracellular trap formation (*Ncf2*, *Cybb*, *Itgb2*, *Selp*, *Clec7a*, and *Casp4*), and delayed apoptosis (*Bcl2a1b*), all of which are associated with lethal endpoints in animal models [40–43]. Neutrophil extracellular trap formation represents a novel mechanism of cell death, wherein neutrophils release DNA fibres carrying MPO and other enzymes in response to infection or stimuli [44]. The protein level of MPO in the BALF of mice subjected to aerosolized intratracheal inoculation was higher than those of mice inoculated intranasally, consistent with the trend observed at the transcript level. ECM is a critical regulator of tissue morphogenesis and repair [45, 46]. Genes related to ECM synthesis were highly expressed in the lungs of mice inoculated intranasally compared to those inoculated via aerosolized intratracheal infection. Hence, we speculated that the mice subjected to intranasal inoculation had already entered the repair phase at 5 dpi.

Conclusion

In conclusion, aerosolized intratracheal infection leads to more severe lung injury and higher viral loads in the lungs compared to intranasal infection, which may be influenced by the initial site of infection, sialic acid receptor distribution, and host innate immunity. Intratracheal inoculation is a better method for modelling severe pneumonia in mice than intranasal infection.

Abbreviations

PR8	Mouse-adapted influenza A/Puerto Rico/8/34 (H1N1)
MMAD	Mean mass aerodynamic diameter
Cy	Cyanine dye
Dpi	Day post-infection
BALF	Bronchoalveolar lavage fluid
GO	Gene ontology

KEGG	Kyoto encyclopedia of genes and genomes
DEGs	Differentially expressed genes
ANOVA	Analysis of variance
i.n.	Intranasal
i.t.	Intratracheal
MPO	Neutrophil myeloperoxidase
ICAM-1	Intercellular cell adhesion molecule-1
PCA	Principal component analysis
ECM	Extracellular matrix

Acknowledgements

Not applicable.

Author contributions

X.J.: Original draft. H.Y.: Original draft. G.Z.: Methodology. C.D.: Software. Z.Z.: Investigation. D.Z.: Project Administration. Q.Y.: Conceptualization, Writing—review and editing. E.D.: Project Administration. All authors have read and agreed to the published version of the manuscript. All authors reviewed the manuscript.

Funding

This work is financially supported by the National Key R&D Program of China (Grant No.2023YFC2605000).

Data availability

The datasets used and/or analysed during the current study are available from the corresponding author on reasonable request.

Declarations

Competing interests

The authors declare no competing interests.

Received: 27 June 2024 / Accepted: 23 September 2024

Published online: 01 October 2024

References

- Krammer F, et al. Influenza Nat Rev Dis Primers. 2018;4(1):3.
- Liu C, et al. Emerging drug design strategies in anti-influenza drug discovery. Acta Pharm Sin B. 2023;13(12):4715–32.
- Uyeki TM, Influenza. Ann Intern Med. 2021;174(11):161–76.
- Grohskopf LA, et al. Prevention and Control of Seasonal Influenza with vaccines: recommendations of the Advisory Committee on Immunization Practices - United States, 2022–23 influenza season. MMWR Recomm Rep. 2022;71(1):1–28.
- Siston AM, et al. Pandemic 2009 influenza A(H1N1) virus illness among pregnant women in the United States. JAMA. 2010;303(15):1517–25.
- Tso WWY, et al. Severity of SARS-CoV-2 Omicron BA.2 infection in unvaccinated hospitalized children: comparison to influenza and parainfluenza infections. Emerg Microbes Infect. 2022;11(1):1742–50.
- Iuliano AD, et al. Estimates of global seasonal influenza-associated respiratory mortality: a modelling study. Lancet. 2018;391(10127):1285–300.
- Belser JA, et al. Comparison of traditional intranasal and aerosol inhalation inoculation of mice with influenza A viruses. Virology. 2015;481:107–12.
- El-Shesheny R, et al. Replication and pathogenic potential of influenza A virus subtypes H3, H7, and H15 from free-range ducks in Bangladesh in mammals. Emerg Microbes Infect. 2018;7(1):70.
- Zhu Z, et al. Infection of inbred BALB/c and C57BL/6 and outbred Institute of Cancer Research mice with the emerging H7N9 avian influenza virus. Emerg Microbes Infect. 2013;2(8):e50.
- Buchweitz JP, Harkema JR, Kaminski NE. Time-dependent airway epithelial and inflammatory cell responses induced by influenza virus A/PR/8/34 in C57BL/6 mice. Toxicol Pathol. 2007;35(3):424–35.
- Rodriguez L, Nogales A, Martínez-Sobrido L. Influenza A Virus studies in a mouse model of infection. J Vis Exp. 2017(127).
- Morales-Nebreda L, et al. Intratracheal administration of influenza virus is superior to intranasal administration as a model of acute lung injury. J Virol Methods. 2014;209:116–20.
- Seo Y, et al. Optimizing anesthesia and delivery approaches for dosing into lungs of mice. Am J Physiol Lung Cell Mol Physiol. 2023;325(2):L262–9.
- Zhao Y et al. Time-Course Transcriptome Analysis of the lungs of mice challenged with aerosols of Methicillin-resistant Staphylococcus aureus USA300 clone reveals inflammatory balance. Biomolecules. 2023. 13(2).
- Wang Y, et al. Mechanism of pulmonary plague biphasic syndrome: inhibition or activation of NF-κB signaling pathway. Future Microbiol. 2023;18:267–86.
- Qiu HY, et al. Aerosolized Zika virus infection in Guinea pigs. Emerg Microbes Infect. 2022;11(1):2350–8.
- Jiao Z, et al. Time-course transcriptome analysis of lungs from mice exposed to ricin by intratracheal inoculation. Toxicol Lett. 2021;337:57–67.
- Eisfeld AJ, et al. C57BL/6J and C57BL/6NJ mice are differentially susceptible to inflammation-Associated Disease caused by Influenza A Virus. Front Microbiol. 2018;9:3307.
- Song Q, et al. C5a receptor1 inhibition alleviates influenza virus-induced acute lung injury. Int Immunopharmacol. 2018;59:12–20.
- Mann PC, et al. International harmonization of toxicologic pathology nomenclature: an overview and review of basic principles. Toxicol Pathol. 2012;40(4 Suppl):s7–13.
- Chomczynski P, Sacchi N. Single-step method of RNA isolation by acid guanidinium thiocyanate-phenol-chloroform extraction. Anal Biochem. 1987;162(1):156–9.
- Deng Q, et al. Particle deposition in the human lung: Health implications of particulate matter from different sources. Environ Res. 2019;169:237–45.
- Koullapis PG, et al. Particle deposition in a realistic geometry of the human conducting airways: effects of inlet velocity profile, inhalation flowrate and electrostatic charge. J Biomech. 2016;49(11):2201–12.
- Sugamata R, et al. Leucomycin A3, a 16-membered macrolide antibiotic, inhibits influenza A virus infection and disease progression. J Antibiot (Tokyo). 2014;67(3):213–22.
- Aratani Y. Myeloperoxidase: its role for host defense, inflammation, and neutrophil function. Arch Biochem Biophys. 2018;640:47–52.
- Kozlovski S, et al. ICAMs are dispensable for influenza clearance and anti-viral humoral and cellular immunity. Front Immunol. 2022;13:1041552.
- Krejtitz JH, et al. Low pathogenic avian influenza A(H7N9) virus causes high mortality in ferrets upon intratracheal challenge: a model to study intervention strategies. Vaccine. 2013;31(43):4995–9.
- Bodewes R, et al. Pathogenesis of Influenza A/H5N1 virus infection in ferrets differs between intranasal and intratracheal routes of inoculation. Am J Pathol. 2011;179(1):30–6.
- Kwon D, et al. Replication and pathogenesis of the pandemic (H1N1) 2009 influenza virus in mammalian models. J Microbiol. 2010;48(5):657–62.
- Tate MD, Brooks AG, Reading PC. Correlation between sialic acid expression and infection of murine macrophages by different strains of influenza virus. Microbes Infect. 2011;13(2):202–7.
- Zhao C, Pu J. Influence of host sialic acid receptors structure on the host specificity of Influenza viruses. Viruses. 2022. 14(10).
- Wang J, et al. Mice fatal pneumonia model induced by less-virulent Streptococcus pneumoniae via intratracheal aerosolization. Future Microbiol. 2024;19(12):1055–70.
- Hao XY, et al. Establishment of BALB/C mouse models of influenza A H1N1 aerosol inhalation. J Med Virol. 2019;91(11):1918–29.
- Bowen LE, et al. Development of a murine nose-only inhalation model of influenza: comparison of disease caused by instilled and inhaled A/PR/8/34. Front Cell Infect Microbiol. 2012;2:74.
- Wiersma LC, et al. Pathogenesis of infection with 2009 pandemic H1N1 influenza virus in isogenic guinea pigs after intranasal or intratracheal inoculation. Am J Pathol. 2015;185(3):643–50.
- De Vleeschauwer A, et al. Comparative pathogenesis of an avian H5N2 and a swine H1N1 influenza virus in pigs. PLoS ONE. 2009;4(8):e6662.
- van den Brand JM, et al. Modification of the ferret model for pneumonia from seasonal human influenza A virus infection. Vet Pathol. 2012;49(3):562–8.
- Luo J, et al. Comparative pathogenesis of H3N2 canine influenza virus in beagle dogs challenged by intranasal and intratracheal inoculation. Virus Res. 2018;255:147–53.
- Corry J, et al. Infiltration of inflammatory macrophages and neutrophils and widespread pyroptosis in lung drive influenza lethality in nonhuman primates. PLoS Pathog. 2022;18(3):e1010395.
- Bordon J, et al. Understanding the roles of cytokines and neutrophil activity and neutrophil apoptosis in the protective versus deleterious inflammatory response in pneumonia. Int J Infect Dis. 2013;17(2):e76–83.

42. Tang BM, et al. Neutrophils-related host factors associated with severe disease and fatality in patients with influenza infection. *Nat Commun.* 2019;10(1):3422.
43. Zhang Y, et al. Neutrophil subsets and their differential roles in viral respiratory diseases. *J Leukoc Biol.* 2022;111(6):1159–73.
44. Narasaraju T, et al. Excessive neutrophils and neutrophil extracellular traps contribute to acute lung injury of influenza pneumonitis. *Am J Pathol.* 2011;179(1):199–210.
45. Schiller HB, et al. Time- and compartment-resolved proteome profiling of the extracellular niche in lung injury and repair. *Mol Syst Biol.* 2015;11(7):819.
46. Clause KC, Barker TH. Extracellular matrix signaling in morphogenesis and repair. *Curr Opin Biotechnol.* 2013;24(5):830–3.

Publisher's note

Springer Nature remains neutral with regard to jurisdictional claims in published maps and institutional affiliations.